JOURNAL OF MATERIALS SCIENCE 29 (1994) 3121–3127

Evaluation of advanced alumina-based ceramic tool inserts when machining high-tensile steel

X. S. LI, I. M. LOW
Materials Research Group, School of Physical Sciences, Curtin University of Technology, GPO Box U 1987, Perth, WA 6001, Australia

Three types of alumina-based ceramic tools (zirconia toughened, titanium-carbide reinforced and silicon-carbide-whisker reinforced) were used to evaluate their cutting performance when machining a high-tensile steel. Experimental studies were carried out at various cutting speeds, feeds and depths of cut, in dry conditions. The cutting performance of the alumina-based ceramic tools was judged by the cutting force produced during the process of machining, by the surface roughness of the workpiece and by the wear rate of the cutting inserts. The influence of the cutting parameters (that is, the cutting speed, feed rate and depth of cut) on the cutting performance is discussed.

1. Introduction

The performance of cutting tools is controlled by a complex interplay of material properties including hot hardness, wear resistance, chemical inertness, fracture toughness and thermal-shock resistance. In general, these are prerequisites for a high-performance cutting tool. Alumina has an excellent hot hardness and a low affinity to most metals or alloys. As such, it has been successfully applied to the machining of cast irons and high-speed finishing operations for steels at high feed rates and shallow depths of cut. The drawbacks of alumina as a tool material are that it lacks fracture toughness and it has a low thermal conductivity which renders it very susceptible to thermal shock [1]. In order to improve the thermo-mechanical properties, alumina-based composites containing 25–40 vol % TiC as a dispersed particulate phase were developed. The addition of a refractory transition-metal-carbide dispersoid much improved the thermal conductivity, and hence the thermal-shock resistance [2, 3]. Not only do Al_2O_3–TiC cutting tools have a thermal-shock resistance that is superior to that of pure-alumina cutting tools, they are also harder and retain their hardness at high temperatures, making them more suitable for finishing operations and the machining of harder steels and cast irons. However, their fracture toughness is still rather poor. Two innovations have been made to increase the fracture toughness of alumina. One is zirconia-toughened alumina [4–6], which consists of partially stabilized tetragonal zirconia particles dispersed in an alumina matrix. The fracture toughness of zirconia-toughened alumina can reach twice that of an alumina matrix. This increase results from a high density of small matrix microcracks absorbing energy by slow propagation. These microcracks are formed by the expansion of ZrO_2 during the tetragonal-to-monoclinic phase transformation [7]. SiC-whisker-reinforced alumina is the other innovation [8, 9]. The whisker reinforcement produces a twofold increase in the fracture toughness of the composite relative to monolithic alumina [10]. The properties of these cutting tools are controlled by factors such as the interface between the matrix and the whiskers, by the size of the whiskers and by the amount of whiskers present in the matrix [11]. SiC-whisker-reinforced alumina has received widespread acceptance in the aerospace industry, where it is regarded as the state-of-the-art cutting-tool material for the finishing and rough machining of superalloys because of its high wear resistance and fracture toughness.

In order to fully utilise the inherent potential of alumina-based ceramic tools in machining modern high-strength materials, it is of value to seek a systematic correlation between the cutting parameters and cutting performance of ceramic tools. The primary objective of this study was to evaluate and compare the cutting performance of these advanced alumina-based ceramic tools and to develop cutting-performance data for them in the machining of high-tensile steel.

2. Experimental techniques

2.1. Cutting-tool materials

Three types of commercial cutting-tool materials were used in this investigation: SN60 and AZ5000, alumina-based materials with additions of zirconia (supplied by the Kyocera Corporation); A65 and HC2, alumina-based materials with additions to titanium carbide (supplied by the Kyocera Corporation and NGK Spark Plugs Co., Ltd respectively); and CC670, a silicon-carbide-whisker-reinforced alumina (supplied by the Sandvik Australia Pty. Ltd). Less than 10 wt % ZrO_2 was present in SN60, while AZ5000 contained more than 10 wt % ZrO_2. More than 50% alumina and less than 50% titanium carbide were present in A65 and HC2. CC670 contained 75 wt % alumina and

0022–2461

TABLE I The ceramic cutting-tool materials used in this study and their properties

Code	Manufacturers' code	Hardness ($H_{v_{10}}$)	Fracture toughness K_{Ic} (MPa $m^{1/2}$)	Average grain size (μm)
ZTA-1	SN60	1650	3.9	5.0
ZTA-2	AZ5000	1800	6.0	1.0
TCA-1	A65	1860	4.1	1.5
TCA-2	HC2	1830	3.8	2.0
SCA	CC670	–	–	–

25 wt % silicon-carbide whisker. The inserts were 12.7 mm^2 square and 4.76 mm thick and conformed to the ISO specification SNGN 120408. The known mechanical properties for all the inserts are shown in Table I.

TABLE II Alloying composition (wt %) of the workpiece material (AISI 4340)

C	Mn	P	S	Si	Ni	Cr	Mo
0.40	0.70	0.035	0.04	0.25	1.85	0.8	0.25

2.2. Workpiece material

Machining tests were conducted on an AISI 4340 steel bar (Rockwell hardness HRB = 95 ± 2). The initial diameter was 150 mm and the length was 660 mm. The alloying composition of the steel is shown in Table II.

TABLE III Cutting conditions during machining operations

Cutting speed (m min^{-1})	300, 400, 500, 600
Feed rate (mm rev^{-1})	0.1, 0.2, 0.3, 0.4
Depth of cut (mm)	0.5, 1.0, 1.5, 2.0
Environment	Dry

2.3. Cutting test

Machining was performed on a Macson lathe. This machine was powered by an 11 kW motor which provided stepwise speed control throughout the range 47–1600 r.p.m (revolutions per minute). The cutting conditions are shown in Table III. The tool holder used was CSBNR2525N43 (NTK) and the tool angles were −6°, −6°, 6°, 6°, 15°, 15° and 0.8°. The orthogonal cutting-force components were measured during turning using a three-axis piezoelectric dynamometer. The signals from the dynamometer were fed through a charge amplifier and recorded on a personal computer. The three force components (namely, the feed force F_x, the thrust force, F_y, and the principal force, F_z) were measured.

At the end of each test, the surface roughness of the workpiece was measured with a Surftest 211 (series 178) surface-roughness tester. The direction of the roughness measurement was perpendicular to the cutting-velocity vector. A total of five measurements of the surface roughness were taken at random on each machined surface.

The tool life of an insert was determined by either the total-tool-failure or the critical-flank-wear (VB = 0.3 mm) criterion. The width of the flank wear land, VB, was measured perpendicular to the major cutting edge, and it was measured from the position of the original major cutting edge. The flank wear was measured with a toolmaker's microscope.

3. Results and discussion

3.1. Flank wear

Figs 1–3 show, respectively, the influence of the cutting speed, the feed rate and the depth of cut on the flank wear of various inserts after 1 min of cutting. The flank wear increased significantly as the cutting speed increased (Fig. 1). The dependence of the cutting temperature on the cutting speed was rather large, since an average temperature increase of two hundred degrees (from 1100 to 1300 °C) has been recorded when changing the cutting speed from 400 to 600 m min^{-1} when machining steel with an alumina ceramic tool [6]. With increasing cutting speed the hardness of the cutting tools decreased due to the rising cutting temperature, so the wear rate of the cutting tools increased. Fig. 1 shows that the flank wear at the lower cutting speed (200 m min^{-1}) was approximately the same for all the inserts, but the flank wear at the higher cutting speed (600 m min^{-1}) was quite different for each insert. The flank wear of SCA was more than twice that of ZTA-2. From this result it can be deduced that the influence of composition and microstructure of cutting tools on the flank wear rate is rather important, especially at high cutting speeds. Fig. 1 also shows that, among these inserts, the wear rate of SCA was the greatest, followed by ZTA-1. The wear rate of TCA-1, TCA-2 and ZTA-2 were nearly the same. The greater wear rate of SCA is probably due to the chemical incompatibility of SiC with iron at high temperatures, which results in the formation of FeSi and FeC. The flank wear on the tools increased with increases in the feed rate (Fig. 2), but the influence of the feed rate on the flank wear was not as great as that of the cutting speed. With increases in the depth of cut from 0.5 to 1.5 mm, the flank wear became larger. However, the flank wear became smaller or remained constant as the depth of cut increased continuously from 1.5 to 2.0 mm. This may be because with increases in the depth of cut the length of the cutting edge in contact with the workpiece increased resulting in a non-linear, and greater, dissipation of the heat produced during cutting.

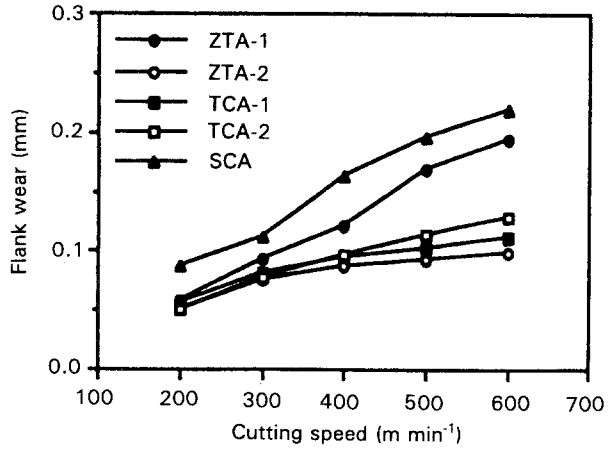

Figure 1 Variation of the flank wear as a function of the cutting speed. Feed rate, 0.2 mm rev^{-1}; depth of cut, 1.0 mm; and time in cut, 1 min.

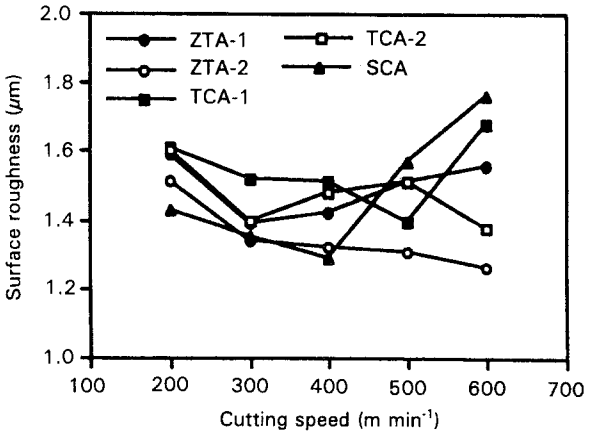

Figure 4 Variation of the surface roughness as a function of the cutting speed. Feed rate, 0.2 mm rev^{-1}; depth of cut, 1.0 mm; and time in cut, 1 min.

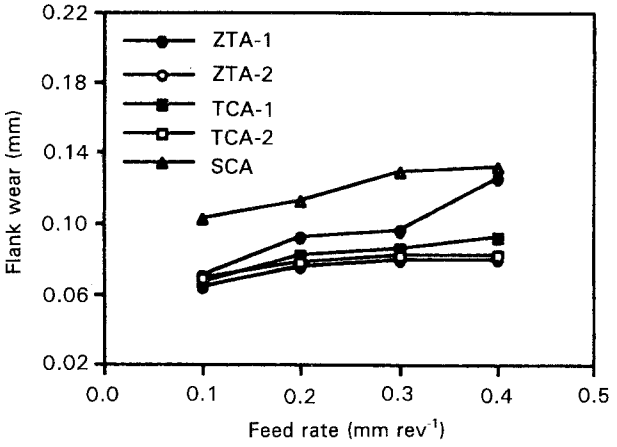

Figure 2 Variation of the flank wear as a function of the feed rate. Cutting speed, 300 m min^{-1}; depth of cut, 1.0 mm; and time in cut 1 min.

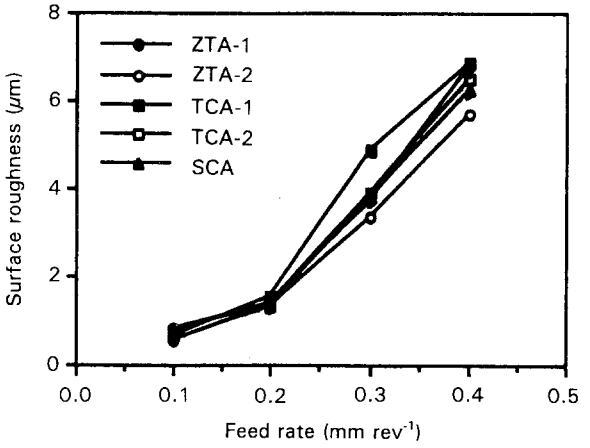

Figure 5 Variation of the surface roughness as a function of the feed rate. Cutting speed, 300 m min^{-1}; depth of cut, 1.0 mm; and time in cut 1 min.

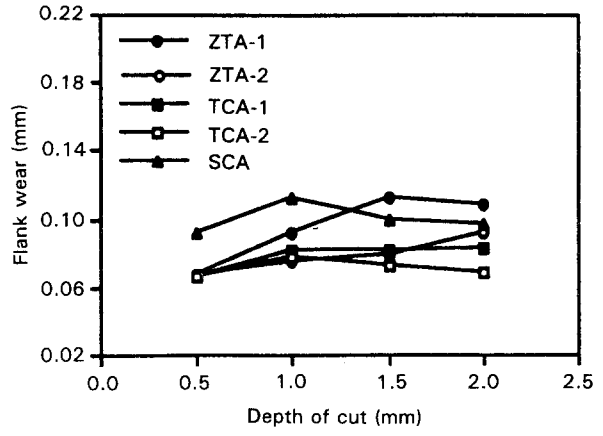

Figure 3 Variation of the flank wear as a function of the depth of cut. Cutting speed, 300 m min^{-1}; feed rate, 0.2 mm rev^{-1}; and time in cut, 1 min.

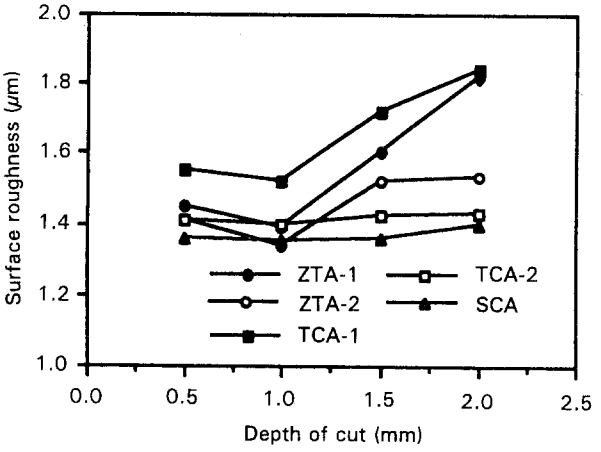

Figure 6 Variation of the surface roughness as a function of the depth of cut. Cutting speed, 300 m min^{-1}; feed rate, 0.2 mm rev^{-1}; and time in cut, 1 min.

3.2. Surface roughness

The influences of the cutting speed, feed rate and depth of cut on the surface roughness of the workpieces are shown in Figs 4, 5 and 6, respectively. From Fig. 4, in all cases, the surface finish improved as the cutting speed increased from 200 to 300 m min^{-1}. With further increases in the cutting speed, the surface finish continued to improve slightly for ZTA-2 and TCA-2, but the surface finish deteriorated slowly for SCA, ZTA-1 and TCA-1. Fig. 5 suggests that the surface finish deteriorated rapidly with increases in the feed rate. The surface finish was very poor at high feed rates. From Fig. 6, the surface roughness decreased and then increased with increases in the depth of cut,

but this variation of the roughness was not great. The feed rate had by far the greatest influence on the surface roughness. The influence of the cutting speed and the depth of cut was lower and it showed little variation within the ranges investigated.

3.3. Cutting force

The influences of the cutting speed, feed rate and depth of cut on the three cutting-force components are summarized in Figs 7–12. The cutting force decreased slightly as the cutting speed increased except for SCA where the cutting force rose as the cutting speed increased. This is probably because the flank wear of the SCA insert increased rapidly with increases in the cutting speed, as mentioned before. The force components also increased rapidly with increases in the feed rate and the depth of cut (Figs 9–12). The influence of the feed rate and the depth of cut on the principal force component, F_z was very similar. The influence of the feed rate on the thrust force component F_y, was larger than that of the depth of cut, but the influence of the feed rate on the feed force component, F_x was smaller than that of the depth of cut. The magnitude of F_z was by far the largest, followed by F_x and then F_y.

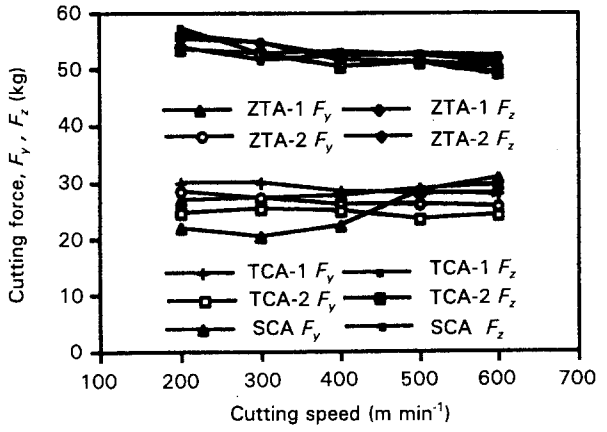

Figure 7 Variation of the cutting force (F_y, F_z) as a function of the cutting speed. Feed rate, 0.2 mm rev^{-1}; depth of cut, 1.0 mm; and time in cut, 1 min

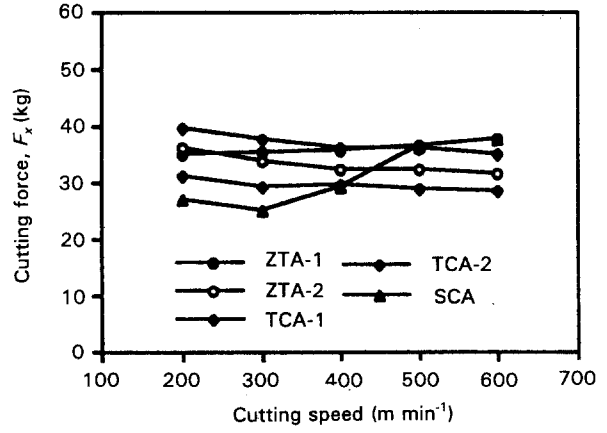

Figure 8 Variation of the cutting force, F_x, as a function of the cutting speed. Feed rate, 0.2 mm rev^{-1}; depth of cut, 1.0 mm; and time in cut, 1 min.

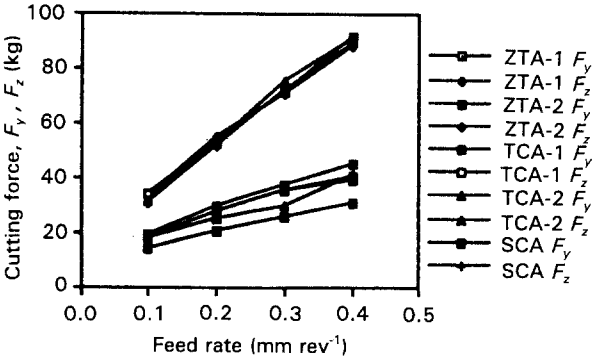

Figure 9 Variation of the cutting force (F_y, F_z) as a function of the feed rate. Cutting speed, 300 m min^{-1}; depth of cut, 1.0 mm; and time in cut 1 min.

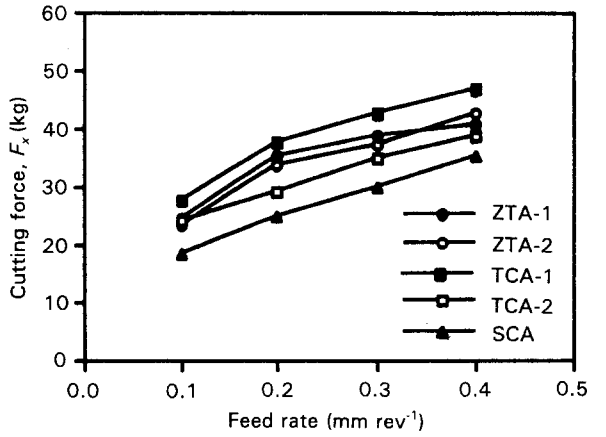

Figure 10 Variation of the cutting force, F_x, as a function of the feed rate. Cutting speed, 300 m min^{-1}; depth of cut, 1.0 mm; and time in cut 1 min.

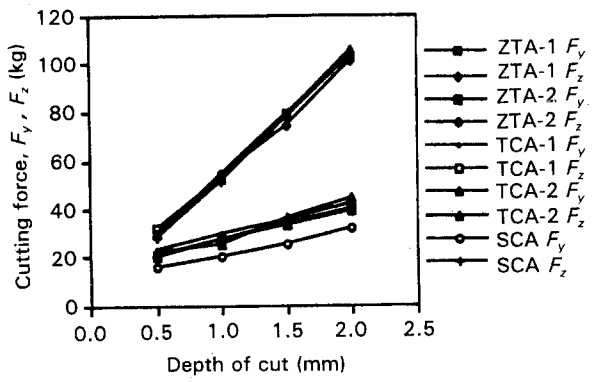

Figure 11 Variation of the cutting force (F_y, F_z) as a function of the depth of cut. Cutting speed, 300 m min^{-1}; feed rate, 0.2 mm rev^{-1}; and time in cut, 1 min.

3.4. Force-component ratios

The variation of the force ratios with the cutting speed, feed rate and depth of cut is shown in Figs 13–18, respectively. Fig. 13 and Fig. 14 show that the cutting speed did not have much effect on the force ratios F_x/F_z and F_y/F_z, respectively and Figs 15 and 16 show that the force ratios decreased with increases in the feed rate. Figs 17 and 18 show the force ratio F_y/F_z fell rapidly, but F_x/F_z rose with increases in the depth of cut. The thrust force component, F_y, had the largest influence on the workpiece dimensional accuracy, thus indicating that reducing F_y is better for

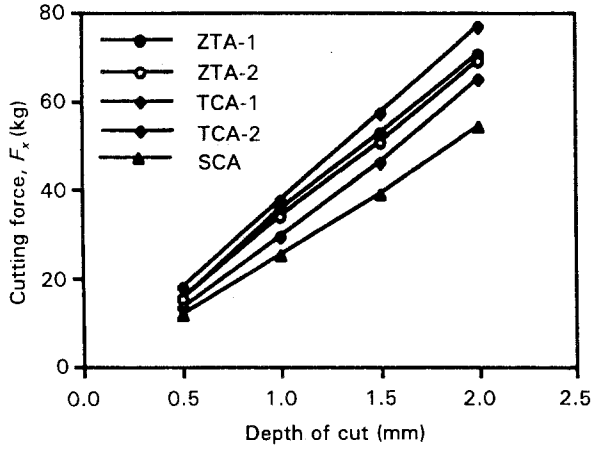

Figure 12 Variation of the cutting force F_x, as a function of the depth of cut. Cutting speed, 300 m min^{-1}; feed rate, 0.2 m rev^{-1}; and time in cut, 1 min.

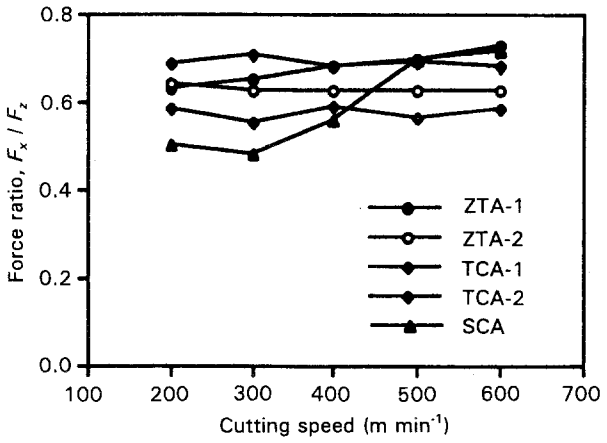

Figure 13 Variation of the force ratio, F_x/F_z as a function of cutting speed. Feed rate, 0.2 mm rev^{-1}; depth of cut, 1.0 mm; and time in cut, 1 min.

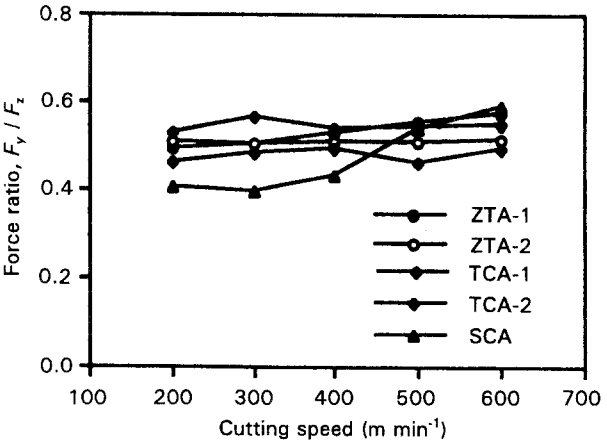

Figure 14 Variation of the force ratio, F_y/F_z, as a function of cutting speed. Feed rate, 0.2 mm rev^{-1}; depth of cut, 1.0 mm; and time in cut, 1 min.

turning with single-point tools. Accordingly, it is recommended that a large depth of cut and a smaller feed rate are used for these tools. From the results of the experiment, it can also be seen that the surface roughness of the workpiece was acceptable under the cutting conditions of a larger depth of cut and a smaller feed rate.

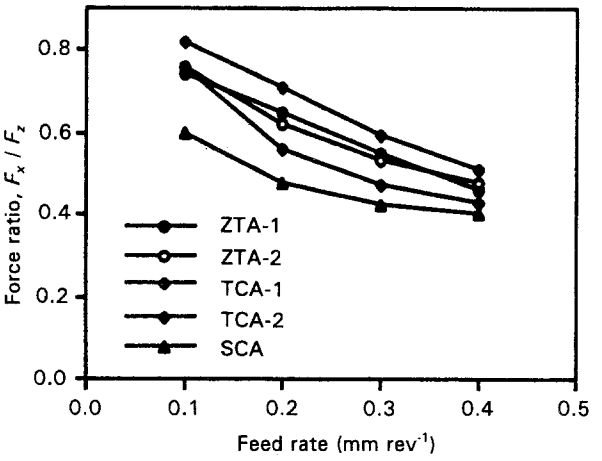

Figure 15 Variation of the force ratio, F_x/F_z, as a function of the feed rate. Cutting speed, 300 m min^{-1}; depth of cut, 1.0 mm; and time in cut 1 min.

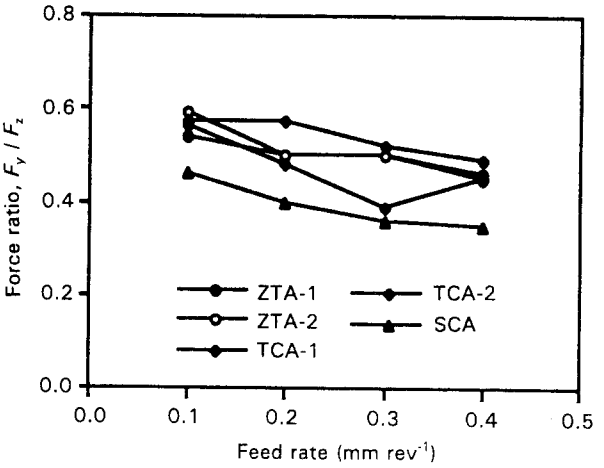

Figure 16 Variation of the force ratio, F_y/F_z, as a function of the feed rate. Cutting speed, 300 m min^{-1}; depth of cut, 1.0 mm; and time in cut 1 min.

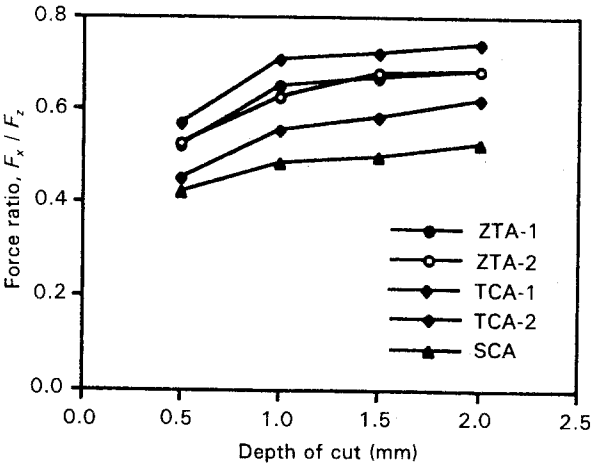

Figure 17 Variation of the force ratio, F_x/F_z, as a function of the depth of cut. Cutting speed, 300 m min^{-1}; feed rate, 0.2 mm rev^{-1}; and time in cut, 1 min.

3.5. The influence of material properties on cutting performance

From Figs 1 to 12, it can be seen that the curves of surface roughness, flank wear and cutting force all exhibited very similar characteristics at various cutting speeds, feed rates and depths of cut. This suggests

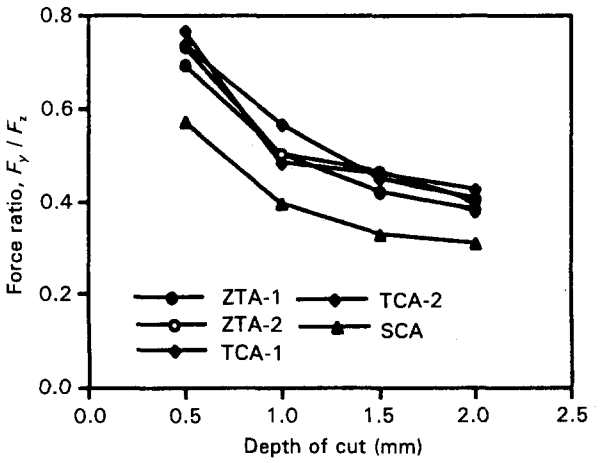

Figure 18 Variation of the force ratio, F_y/F_z, as a function of the depth of cut. Cutting speed, 300 m min^{-1}; feed rate, 0.2 mm rev^{-1}; and time in cut, 1 min.

that cutting parameters have a similar influence on the cutting performance of these alumina-based tools. Comparing two zirconia-toughened alumina tools, it can be seen that the values of the surface roughness, flank wear and cutting force for ZTA-2 are less than those for ZTA-1. This suggests that the cutting performance of a tool depends on its structure, properties and cutting conditions [12, 13]. A tool with high hardness, good fracture toughness and a fine-grained structure (for example, ZTA-2) will have a better flank wear resistance and surface finish than a tool with inferior properties (ZTA-1, for example). However, this properties–performance link is only very obvious at heavy cutting conditions (that is greater cutting speeds, feed rates and depth of cut) and it is less apparent under light cutting conditions (that is reduced cutting speeds, feed rates and depths of cut). In short, ceramic cutting inserts with improved mechanical properties can have an advantage under heavy cutting conditions. Comparing the two titanium-carbide-reinforced alumina tools, in Table I, it can be seen that the cutting performance of both tools was nearly the same, which is consistent with their similar mechanical properties. Comparing the tools based on zirconia and titanium carbide, the cutting performance of TCA-1 and TCA-2 was better than that of ZTA-1, but slightly worse than that of ZTA-2. At low cutting speeds, the cutting performance of SCA was nearly the same as that of other tools, but under high cutting speeds the cutting performance of SCA was much inferior to the other tools. The cost of the SCA is also higher than that of other tools, so silicon-carbide-whisker-reinforced alumina is not recommended for machining AISI 4340 high-tensile steel.

4. Conclusions

The following conclusions are based on turning tests carried out with various commercial alumina-based cutting tools on high-tensile steel (AISI 4340) at cutting speeds ranging from 200 to 600 m min^{-1}, feed rates ranging from 0.1 to 0.4 mm rev^{-1} and depths of cut ranging from 0.5 to 2.0 mm.

1. With increases in the cutting speed, the flank wear of the tools increased significantly. The order of the influence of cutting parameters on the flank wear was: cutting speed, feed rate and depth of cut.
2. With increases in the feed rate, the workpiece surface roughness increased significantly. The influence of the cutting speed on the workpiece surface roughness was complex and it was quite dependent on the material properties of the cutting tools. For the tools with higher hardnesses and fracture toughnesses, the workpiece surface roughness decreased as the cutting speed increased. But for the tools with lower hardnesses and fracture toughnesses, the workpiece surface roughness increased as the cutting speed increased.
3. The principal force, F_z, remained fairly similar for all the tools subjected to identical cutting conditions. However, the feed force, F_x and the thrust force, F_y, showed distinct variations under identical cutting condition. From this result it can be deduced that the material properties of the cutting tools have a greater influence on the feed force and thrust force than on the principal force.
4. The force ratio F_y/F_z decreased and the force ratio F_x/F_z rose with increases in the depth of cut.
5. For the three types of alumina-based cutting tools investigated, under light cutting conditions (that is, lower cutting speeds, feed rates and depths of cut), the cutting performances were similar, but under heavy cutting conditions (that is, higher cutting speeds, feed rates and depths of cut) ZTA-2, TCA-1 and TCA-2 demonstrated better cutting performances than ZTA-1 and SCA.
6. The results indicate that both types of alumina-based tools (zirconia toughened and titanium-carbide reinforced) can be used effectively under the cutting conditions of smaller feed rates and larger depths of cut. Silicon-carbide-whisker-reinforced alumina is however not recommended for machining AISI 4340 high-tensile steels.

Acknowledgements

X. S. Li thanks the Commonwealth Government of Australia and AINSE for financial support in the form of a scholarship and a research supplement, respectively. I. M. Low is grateful to the Australian Research Council for funding under the Small Grants and Mechanism B schemes. The authors also thank Kyocera Corporation, NGK Spark Plugs Co., Ltd and Sandvik Australia Pty. Ltd for providing the ceramic cutting inserts. Thanks are also due to Professor B. O'Connor and to Professor J. Wager for their useful comments.

References

1. S. T. BULJAN, and V. K. SARIN, "Cutting tool materials" (American Society for Metals, Metals Park, Ohio, 1981) p. 193.
2. M. FURAKAWA, O. NAKANO and Y. TAKASHIMA, *Int. J Refractory Hard Metals* 7 (1988) 37.
3. M. FURAKAWA, *Amer. Ceram. Soc. Bull.* **62** (1983) 1384.
4. L. J. SCHIOLER and R. N. KATZ, *Ceram. Eng. Sci. Proc.* **6** (1985) 822.

5. B. MONDAL, A. B. CHATTOPADHYAY, A. VIRKAR and A. PAUL, *Wear* **156** (1992) 365.
6. N. NARUTAKI, Y. YAMANE and K. HAYASHI, *Annals CIRP*, **40** (1991) 49.
7. N. CLAUSSEN, *J Amer. Ceram. Soc.* **59** (1976) 49.
8. A. R. THANGARAJ and K. J. WEINMANN, *Trans. ASME J. Engng Indust.* **114** (1992) 301.
9. E. R. BILLMAN, P. K. MEHROTRA, A. F. SHUSTER and C. W. BEEGHLY *Amer. Ceram. Soc Bull.* **67** (1988) 1016.
10. G. C. WEI and P. F. BECHER, *ibid.* **64** (1985) 296.
11. J. VIGNEAU, P. BORDEL and A. LEONARD, *Annals CIRP* **36** (1987) 13.
12. X. S. LI, I. M. LOW, J. G. WAGER, D. S. PERERA and B. H. O'CONNOR, Proceedings of the Internatioal Conference on Advanced Composites, Fabrication, Processing, Properties, Performance, Design and Applications, 15–19 February 1993, University of Wollongong, Australia, in press.
13. X. S. LI and I. M. LOW, *J. Mater. Sci. Lett.*, in press.

Received 16 September 1993
and accepted 10 January 1994